The Design and Use of Electromagnetic Acoustic Wave Transducers (EMATs)

by B. W. Maxfield and C. M. Fortunko

Abstract

Electromagnetic acoustic wave transducers (EMATs) are a broad class of ultrasonic transducers that can generate bulk shear and longitudinal waves, Rayleigh, Lamb, and general surface acoustic waves in metals with no mechanical (fluid) coupling. EMATs have a number of advantages over conventional piezoelectric transducers, as well as the general disadvantage of larger insertion loss. Proper sensor and electronics design permits good signal-to-noise levels to be achieved, thereby enabling one to exploit the advantages of EMATs.

The absence of a fluid couplant makes it possible to design transducers that operate at elevated temperatures (1200°F [649°C] has been realized to date) and scan at high speeds. The operating characteristics of EMATs can be reproduced from one unit to another quite easily, making them useful as ultrasonic standards. No poling is involved in EMATs, so their performance is relatively free from aging effects. EMATs also offer essentially new possibilities in ultrasonic wave generation because shear-horizontal (SH) waves, which are easily generated with EMATs, must otherwise be generated with rigidly bonded transducers. Shear waves of any desired polarization can be generated perpendicular to the surface. These can be used for single transducer thickness gaging. The direction of angle-beam shear and longitudinal waves can be controlled electronically (by controlling the frequency) and hence offer new approaches to test development. To realize any particular set of these special features and advantages, careful attention must be given to the EMAT design. Because the insertion loss of EMATs can be as much as 40 dB greater



Bruce Maxfield received his B.Sc. degree in physics from the University of Alberta in 1961 and the Ph.D. degree in physics from Rutgers University in 1964. He then joined Cornell University as a research associate. In 1966, he was appointed assistant professor and was appointed as senior research associate in 1972. He joined the Nondestructive Evaluation Section at Lawrence Livermore National Laboratory in 1976 as R&D group leader and became NDE section leader in 1981. In 1980, he founded Materials Engineering Associates (Calif.), Ltd., to exploit EMAT technology

and is currently president of MEA(Calif.), Ltd. He has published over 50 papers in a variety of science and engineering areas.

than for comparable piezoelectric configurations, correct impedance matching on generation and reception becomes very important. Different drivers must be used for EMATs because they are current-operated devices for the generation of ultrasonic waves. When properly designed and instrumented, an EMAT-based ultrasonic system can be used for thickness gaging under high loss conditions, and defects at least as small as 0.030 in. (0.76 mm) can be detected reliably. This paper provides the details needed to design SH wave and longitudinal and shear bulk wave EMATs using either permanent magnets or electromagnets to provide the bias field. Additional considerations needed for high temperature, high speed, and other practical inspection situations are described.

INTRODUCTION

The basic theory that describes elastic wave generation via magnetic forces on induced or eddy current distributions has been treated very thoroughly for all wave models. ¹⁻⁴ These theoretical treatments provide the basis for interpreting numerous measurements. Agreement is generally good, giving one a high degree of confidence that the theory does, indeed, include all relevant terms.

The main objective of this paper is not to discuss theoretical treatments, but rather to describe how practical devices for different kinds of elastic wave generation may be constructed and used for making measurements. This does not mean that the theory is not important; it is obviously an essential element in understanding device performance. There are, however, several important aspects of the functioning of EMATs that are not part of the usual underlying theoretical description. These features will be emphasized in this paper.

ELASTIC WAVE GENERATION

The most widely used methods for elastic wave generation rely upon some form of electromechanical conversion. In a piezoelectric generator, an applied voltage charging a capacitive element produces an internal electric field having approximately the same time dependence as the applied voltage. In piezoelectric materials, the force associated with this electric field causes the interatomic spacing to change slightly. This elastic disturbance will generally propagate. If the piezoelectric material is mechanically coupled to another elastic body, then the elastic disturbance in the piezoelectric material will generate an elastic wave in that elastic body. This wave will bear some resemblance to the voltage originally applied. If a magnetostrictive generator is used, then an applied magnetic field from an inductive element produces an elastic wave in a mechanically coupled elastic body.

In electromagnetic acoustic-wave generation (EAG), magnetic forces on an electrical-induced current distribution in a metal couple to the atomic lattice via electron-ion and electronimpurity collisions.5 Thus, a current applied to an inductive element placed in proximity to a metal surface induces eddy currents that experience a magnetic or Lorentz force. This force generates an elastic disturbance that is usually a precise temporal reproduction of the magnetic force. Note that for EAG, the electromechanical conversion takes place directly within the eddy current skin-depth; that is, no mechanical coupling to an elastic body is needed. Thus, the metal surface is its own transducer, and there exists no acoustic impedance mismatch to its transducer. In contrast, an elastic wave generated by piezoelectric or magnetostrictive means must be mechanically coupled into the material one wishes to evaluate. Mechanical resonances and elastic damping in the transducing element and coupling material will influence, sometimes dramatically, the elastic wave that gets coupled out of the transducing element and into the elastic body under study.

Herein lies the main and often the only important difference between transducers based on EAG and mechanically coupled transducers; namely, that transduction takes place in the elastic body under study. In addition, EAG is a linear, reciprocal process. Consequently, it works in an analogous manner as a receiver (the elastic wave in the metal produces an electric field that is sensed by the coil near the surface). Henceforth, this entire class of generators and receivers will be referred to as EMATs.

The price that one pays for this freedom from mechanical coupling is often a reduced signal level. Note that level has been used and not signal-to-noise ratio (S/N). One can frequently achieve an S/N comparable to that obtainable using the more conventional piezoelectric approach. To accomplish this, however, considerable attention must be given to both the EMAT design and the measurement system characteristics.

There are also some situations where S/N is not the over-

riding concern, for example, in thickness gaging or the mapping of large defects in plates and welds. Here, the high speed achievable with EMATs on unprepared surfaces may be a much more important factor.

Other situations where EMATs will prove valuable relate to circumstances where coupling conventional transducers is either difficult or impossible, for example, at very high temperatures or in applications involving large neutron or gamma fluxes. Under these conditions, fluid couplants can no longer be used. Mechanical coupling is usually accomplished by high pressure, momentary contact with the surface. With EMATs, pulsed electromagnets and sensor coils have been made that operate at 1200°F (649°C) continuously with the possibility of continuous operation eventually extending to at least as high as 2200°F (1204°C). Also, conventional electromagnets with water-cooled face plates can be used near surfaces at least as hot as 1200°F (649°C). EMATs are also quite radiation resistant.

The next three sections describe different classes of EMATs, how they should be used in a measuring system, and some aspects of the driving and receiving electronics that the authors have found to be important.

SURFACE WAVE AND ANGLE-BEAM EMATS

To generate surface or angle-beam elastic waves, it is necessary to have a spatially periodic driving force at the free surface. This is accomplished by using a periodic induced current, a periodic magnetic field, or some combination of these two approaches. Practical periodic magnetic fields for use in EMATs and having a spatial frequency of 0.1 to 1 cm have only been produced using permanent magnets. Considerable work has been done with EMATs using periodic permanent magnets (PPMs) and a uniform induced current sheet. ^{6,7} This configuration produces a driving force that is always parallel to the surface and perpendicular to the direction of propagation, regardless of the propagation angle. Consequently, a PPM EMAT generates a pure SH wave; this EMAT configuration will be discussed in more detail in the section titled "SH Wave EMATs."

Another quite novel means of generating an SH wave uses spatial variation of both the magnetic field and the induced current. Configurations of this EMAT that have been tried so far exhibit a greater insertion loss than the PPM EMAT, but this new design has the advantage of using the higher fields achievable with electromagnets.

The meander line or surface acoustic wave generator placed in a uniform magnetic field is another means of generating surface and angle-beam elastic waves. 4,9,10 In this case, however, the particle motion is only perpendicular to the propagation direction for wave propagation parallel to the surface. At all nonzero propagation angles, both shear and longitudinal waves are generated. These EMATs are discussed in the section titled "Meander Line EMATs."

SH Wave EMATS

When searching for defects in weldments and similar structures, it is desirable to maximize collimation of the ultrasonic beam in the direction of the flaw. This can be accomplished in two ways: (1) using synthetic aperture processing and (2) using an SH wave EMAT with the desired beam shape characteristics. In practice, to satisfy system design considerations, the desired collimation of the ultrasonic beam is usually obtained by a combination of both approaches.

This section emphasizes the details of SH wave EMAT design that are needed to obtain the desired beam shape characteristics and, simultaneously, to reduce the effect of unwanted ultrasonic and electromagnetic interferences.

Figure 1 shows a primitive EMAT element composed of a wire carrying a dynamic current, I_{ω} , and a source of strong magnetic bias field, H_{\circ} . The current I_{ω} induces dynamic eddy currents, J_{ω} , in the surface of the metal conductor. The presence of the strong magnetic bias field, H_{\circ} , causes deflection of the

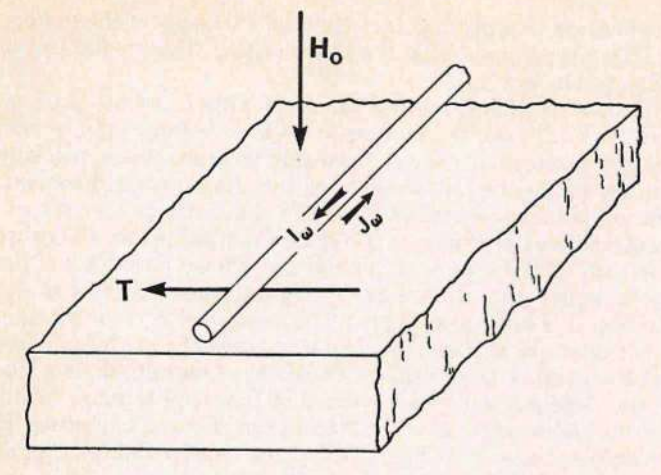
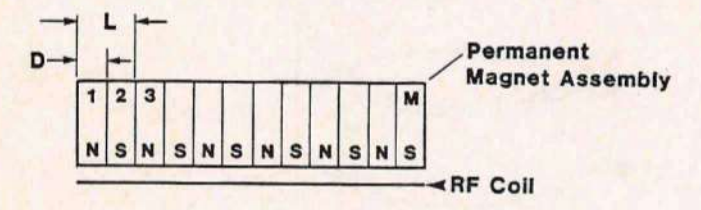


Figure 1—An elemental EMAT consisting of a wire in a magnetic field placed near a metal surface.

moving electrons in a direction defined by the vector cross-product of J_{ω} and H_{o} . The resultant Lorentz body forces, T, generate ultrasonic energy that propagates into the bulk of the metal away from the wire. Of course, the polarization of such signals depends on the direction of the static field with respect to the free surface. (In this paper, the subject of generating ultrasonic energy using magnetostrictive transduction mechanisms is not discussed.)

The primitive elemental transducer depicted in Fig. 1 is not often very useful for practical measurements. First, it is not very efficient because of the practical difficulties of efficiently matching isolated wire radiators to transmitter-amplifiers and receiver-preamplifiers in the frequency band of 0.1 to 10 MHz normally used in flaw detection. Second, the radiation pattern generated by such a primitive EMAT exhibits cylindrical symmetry when SH waves are generated. Cylindrical radiation patterns are not useful for inspecting butt welds in plates or for most other nondestructive evaluation (NDE) problems. Clearly, a practical EMAT must generate most of the signal in the general direction of the flaw and discriminate against signals that can propagate along directions near the normal to the plate.

In the past, a number of different EMAT configurations have been proposed. 11-14 In the majority of applications that involved SH waves, extensive use was made of PPM EMATs of the general type depicted in Fig. 2. It is clear that this EMAT can be constructed by superposing a number of the primitive EMATs shown in Fig. 1. However, in Fig. 2, the static magnetic field sources are arranged periodically along the conductor carrying the dynamic current, I... When two oppositely polarized rows



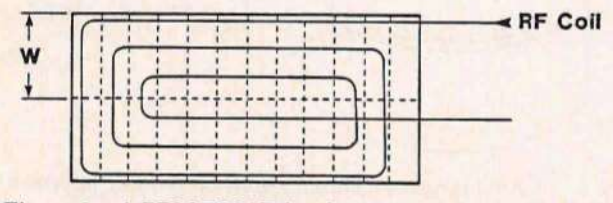


Figure 2—A PPM EMAT for the generation of pure SH waves.

of magnets are used, the conductor can be arranged in the form of an elongated spiral coil, as shown schematically in Fig. 2.

Factors governing the beam-forming characteristics (e.g., directivity) of PPM EMATs and the principles of the transduction mechanisms have been described extensively.³ In the sagittal plane (i.e., the plane normal to the surface of the plate and parallel to the principal propagation direction), the directivity pattern of a PPM EMAT can be determined approximately from the relation:

(1)
$$DF(\phi) = \left\{ \frac{\pi}{2} \frac{\sin x}{x} \right\} \left\{ \frac{\sin \left[\frac{M}{2} (x - \pi) \right]}{\sin \left[\frac{1}{2} (x - \pi) \right]} e^{-j\frac{M\pi}{4}} \right\}$$

where $x=\frac{2\pi D}{\lambda}\sin\phi$, λ is the bulk ultrasonic wavelength, and the angle ϕ is defined by the ray from the center of the PPM EMAT to an observation point and the normal to the surface of the plate (see Fig. 3). As shown in Fig. 2, the PPM EMAT is composed of a periodic array of M permanent magnets (some properties of these magnets are discussed later) with a period L=2D and half-width W with a coil that is always placed between the magnet assembly and the metal surface. In practice, a spacer of thickness S (not shown in Fig. 2) is inserted between the magnets to reduce eddy current losses; consequently, one has L = 2(S+D).

The PPM EMAT of Fig. 2 is composed of essentially independent cells that are connected in parallel electrically and in series acoustically. As a consequence, the PPM EMAT can be viewed as the ultrasonic equivalent of an electromagnetic "end-fire" antenna. This fact is reflected in Equation 1, which can be interpreted as a product of element ("structure") and array ("form") factors. (For clarity, the element and array factors are isolated using brackets.) Narrow beamwidths can only be realized when the EMAT is driven electrically by a tone-burst that is at least M/2 cycles long. Then, the principal beam direction can be determined from:

(2)
$$\phi = \arcsin(\lambda/2[D+S]),$$

where ϕ is the angle defined previously and in Fig. 3.

The "end-fire" properties of the PPM EMAT shown in Fig. 2 can be verified experimentally using the calibration configuration shown in Fig. 3, namely, a 153 mm radius, 203 mm wide aluminum test-block with a semicylindrical cross section. In the configuration of Fig. 2, the PPM EMAT under test (in this case, the transmitter EMAT) is placed symmetrically at the intersection of the two symmetry planes of the semicylindrical test block. A second EMAT, such as shown in Fig. 3, is used as a probe or receiver. This receiver EMAT is of a design described in the section titled "Bulk Wave Generation Normal to a Metal Surface" and has maximum sensitivity to shear

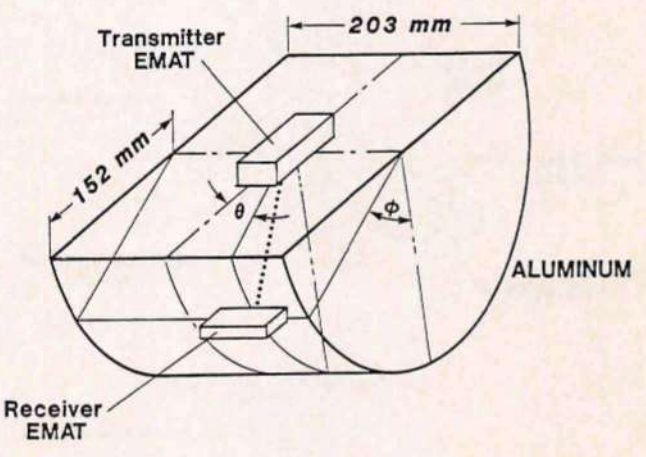


Figure 3—An experimental configuration that can be used for mapping EMAT directivity patterns.

waves that propagate along the normal to the surface. As a result, it is very useful in diagnosing the performance characteristics of the more complicated PPM EMATs. The angles ϕ and θ , which define the coordinates of the observation point, are also shown in Fig. 3.

Although the SH wave EMAT shown in Fig. 2 exhibits the desired directivity characteristics, it suffers from excessive sensitivity to electromagnetic interferences. A better design that uses two separate radio frequency (rf) coils to induce eddy currents is shown in Fig. 4 for the case of M=4. Note that the coils are placed symmetrically with respect to the sagittal plane (not shown) and are connected in series electrically to increase the electrical input impedance. One of the coils is wound in the clockwise direction while the other is wound counterclockwise. This winding arrangement is used to reduce the sensitivity of the EMAT to electromagnetic interferences and to minimize direct electromagnetic cross talk between adjacent sections. To maintain phase coherence in the SH wave that is generated, four rows of permanent magnets are used. The fourmagnet structures are also arranged symmetrically with respect to the sagittal plane but are polarized to maintain mirror symmetry with respect to that plane.

Figure 4 shows all of the essential EMAT components except for a thin (120 μ m thick) 304-type stainless steel or other material face plate that is used in practice to protect the EMAT coils from damage. The individual magnets are separated using 0.5 mm thick glass-epoxy spacers to reduce eddy current flow in the magnets. A central web made of 1.3 mm thick glass-epoxy is used to separate the four rows of magnets into two assemblies, one associated with each of the coils. In addition, 0.5 mm thick glass-epoxy spacers are placed between the magnets and 3.7 mm thick soft-iron plates that serve as magnet-keepers and shunts.

For operation in the 400 to 500 kHz frequency region, the authors used magnets 5 mm thick along the polarization direction, 3.3 mm along the surface wave propagation direction, and 8 mm wide. With the spacers, this gives a period L = 7.6 mm. Each elongated spiral coil contains 24 turns of 32 American wire gage (AWG) copper magnet wire. At 500 kHz, the electrical input impedance is (19 + 15j) ohms (Ω); j = $\sqrt{-1}$. This is a relatively large impedance level that is intermediate between the high impedance levels that are optimum for field-effect transducer (FET) input receiver-preamplifiers (typically 600 Ω) and the low impedance levels required by the transmitter (less than 1 Ω). It can, therefore, be conveniently raised

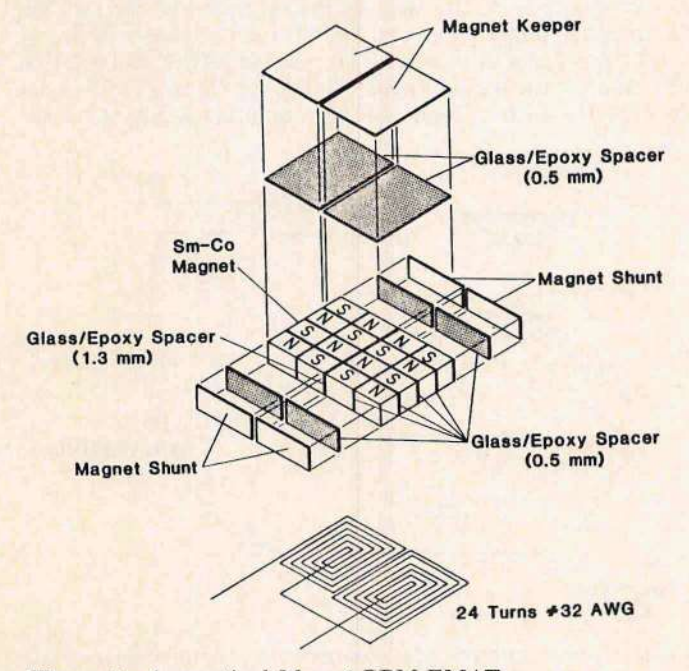


Figure 4—A practical M = 4 PPM EMAT.

or lowered to maximize the electrical efficiency of the system. (This topic is covered in the section titled "Design and Use of EMAT Drivers.")

It can be difficult to use the same EMAT as both a transmitter and receiver of ultrasonic waves because of the long receiver saturation recovery time that one encounters, specially at low frequencies. In these situations, the preferred configuration is composed of two EMATs that are positioned symmetrically with respect to a common sagittal plane. To ensure that the EMATs are spaced uniformly above the surface of the plate under inspection, a gimble mount such as the one shown in Fig. 5 is employed. This mount uses two axes of rotation that intersect at 90 degrees and are parallel to the free surface of the plate. A third degree of freedom is permitted along the axis perpendicular to the surface of the plate to allow lifting of the transducer case. The transducer case and mounting arrangement shown in Fig. 5 have functioned reliably on most unprepared surfaces.

Figures 6 through 8 show radiation patterns in the sagittal plane of the SH wave EMAT shown in Fig. 4. In particular, radiation patterns are shown for 400, 500, and 700 kHz when the EMAT is driven by a tone-burst signal of 3-cycles duration. Some figures also show the actual appearance of the transmitted ultrasonic waveforms as measured using the test setup shown in Fig. 3.

The large angular width forward lobe goes from being about 30 degrees from the surface at 400 kHz to around 60 degrees

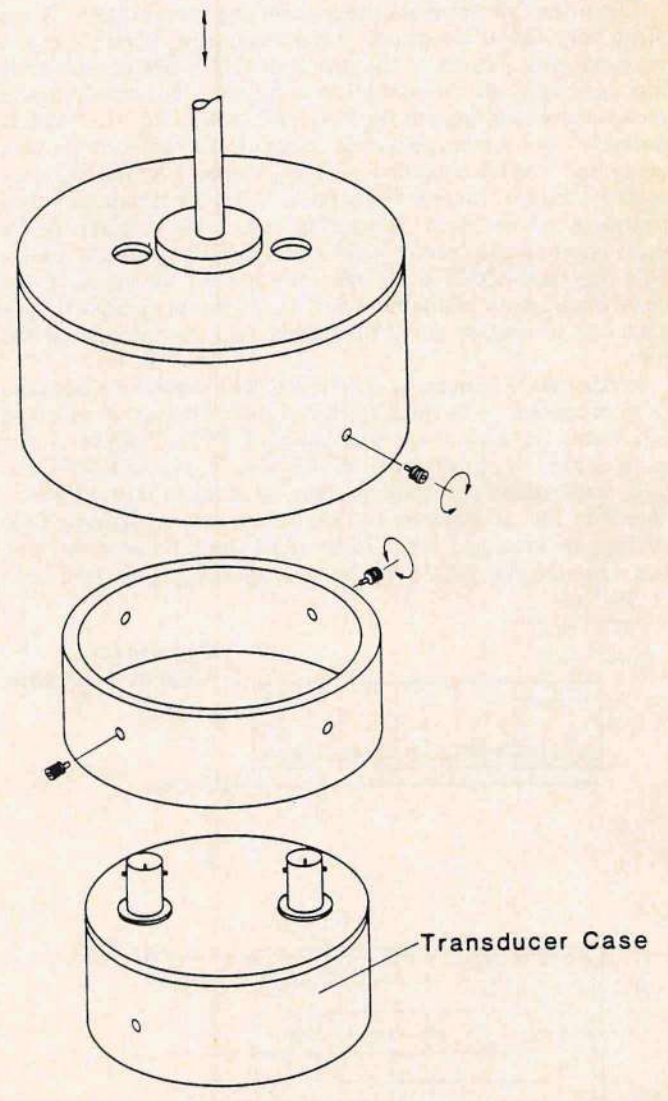


Figure 5—A gimbal mount that can hold two EMATs in proper alignment for pitch-catch measurements.

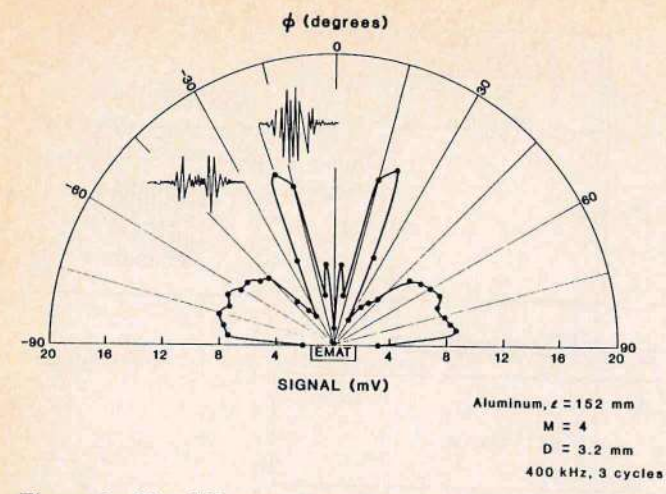


Figure 6—The SH wave directivity pattern of the EMAT in Fig. 4 for $f_0 = 400 \text{ kHz}$.

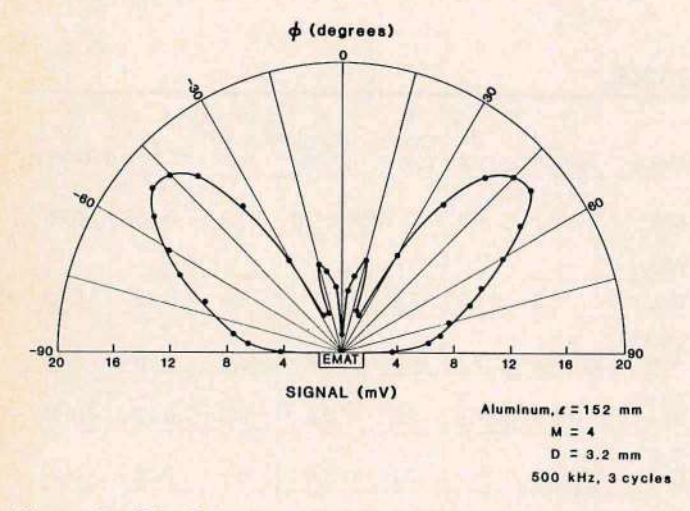


Figure 7—The SH wave directivity pattern of the EMAT in Fig. 4 for $f_0 = 500 \text{ kHz}$.

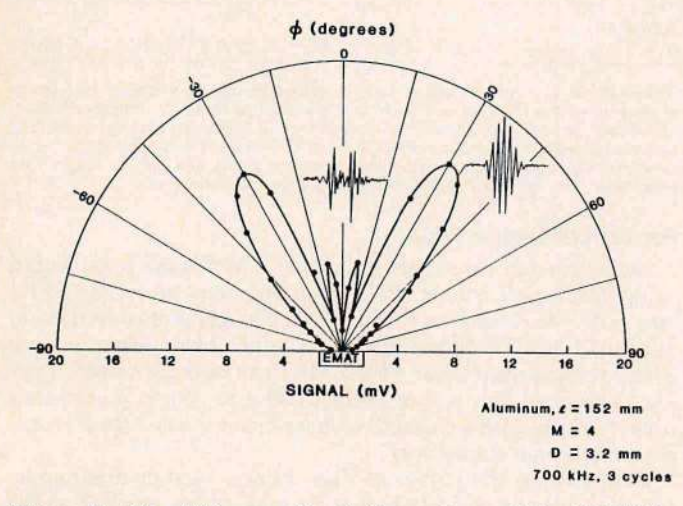


Figure 8—The SH wave directivity pattern of the EMAT in Fig. 4 for $f_0 = 700 \text{ kHz}$.

from the surface at 700 kHz. These shapes are about as expected from Equation 1, except at the lower frequencies the side lobes have a larger amplitude. The relative amplitude of these side lobes increases with the tone-burst pulse length. These nonideal features are associated with diffraction and end effects in the SH wave transducer.

Meander Line EMATs

Figure 9 is a schematic representation of a meander line (ML), serpentine coil, or surface acoustic wave EMAT. These have been well described theoretically and used as Lamb wave and angle-beam EMATs. 3.4.15-17 The directivity pattern is somewhat different from that for SH waves given by Equation 1. For wavelengths shorter than 2D, where D is the conductor element spacing shown in Fig. 9, both shear vertical (SV) and longitudinal (L) waves are generated. This opens the possibility for angle-beam L waves as well as shear waves. One significant advantage of ML EMATs is that electromagnets can be used to produce H₀ and hence give larger signal levels than are available using PPM EMATs. They are readily adaptable for use with magnetic and nonmagnetic materials.

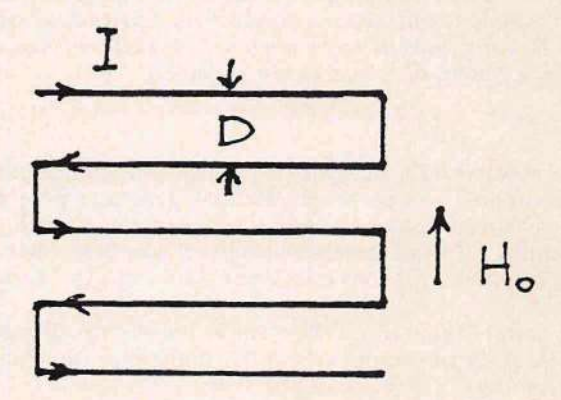


Figure 9—The schematic representation of a ML EMAT, two periods in length.

BULK WAVE GENERATION NORMAL TO A METAL SURFACE

Bulk waves propagating normal to the surface are generated by force distributions that are reasonably uniform and at least many wavelengths in the transverse dimensions. This type of EMAT can be used in a standard pulse-echo mode where the same transducer acts as both generator and receiver or in the through-transmission mode where separate transducers are used as the generator and receiver. Applications include thickness gaging and defect detection. Because of the larger insertion loss of EMATs over piezoelectric transducers, they are less sensitive to small defects. Reliable detection of direct backscattered signals from defects smaller than about 1 mm can be very difficult. If, however, the part geometry is such that a good back surface reflection can be obtained, then the loss-ofback reflection technique can be applied. Even small defects can scatter measurable amounts of ultrasonic energy out of the main beam, and this shows up as a reduced back-reflection signal. Although defects can be detected this way, it is difficult to characterize them as to size and shape. Of course, a throughtransmission technique is also sensitive to small amounts of energy scattered out of the main beam, but it also suffers from the same limitations on quantitative interpretation.

The authors have also found that EMATs using electromagnet bias fields can be adapted to high-temperature, contactless measurements (at least up to 1200°F [649°C] and probably to 2200°F [1204°C]). Bulk wave EMATs can be made using either steady or pulsed field electromagnets as well as permanent magnets.

When an inductive element (coil), whose size is many wavelengths in each direction parallel to the surface, is placed near a metal surface in a magnetic field, an elastic wave is generated that propagates perpendicularly away from the surface. If the surface is rough, then beam distortion will result in much the same manner as for a conventional fluid-coupled beam. The main difference is that EMATs usually allow one to maintain the coupling easier on rough surfaces. Figure 10 shows two

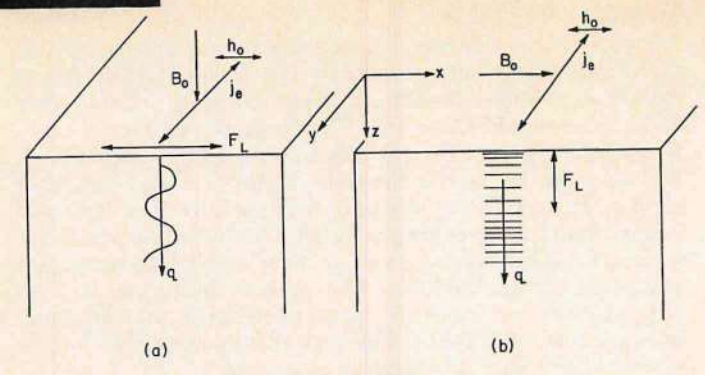


Figure 10—The magnetic field and current configuration required to generate (a) shear waves and (b) longitudinal waves. When B₀ is inclined at some angle to the surface, then both shear and longitudinal waves are generated.

special cases with the magnetic field perpendicular and parallel to the surface. The perpendicular case generates pure shear waves with particle motion parallel to the driving force, F_L , and the parallel field case generates longitudinal waves. Many different coil geometries, such as those shown in Fig. 11, can be used.

For both of these cases, the transfer impedance, defined by the ratio of the coil output voltage, V_o , to the excitation current, I, is given by

(3)
$$Z_T = \frac{V_o}{I} = \frac{B^2 G^2 A}{Z_A}$$
,

where B is the proper magnetic field component (perpendicular or parallel), G is a factor determined by coil geometry and winding density (but which is roughly the turns per unit length), A is the coil active area (see Fig. 12), and Z_A is the acoustic impedance for the mode being considered (shear or longitudinal). Strictly speaking, this expression is only valid for the acoustic wavelength, λ , greater than the electromagnetic skindepth defined by

$$\delta = (2\rho/\mu\omega)^{1/2},$$

where ρ is the electrical resistivity, μ the magnetic permeability, and $\omega = 2\pi f$ is the angular frequency of the induced currents. An additional restriction requires that the surface be unconstrained, although an analogous expression can be derived for a constrained surface. Values of δ and λ at a few frequencies are given for some useful materials in Table 1.

Very good agreement between calculated and measured values of the transfer impedance is obtained.⁵ In addition to giving confidence in understanding the operation of EMATs, this opens the possibility of using EMATs for either primary or secondary standards in ultrasonics.

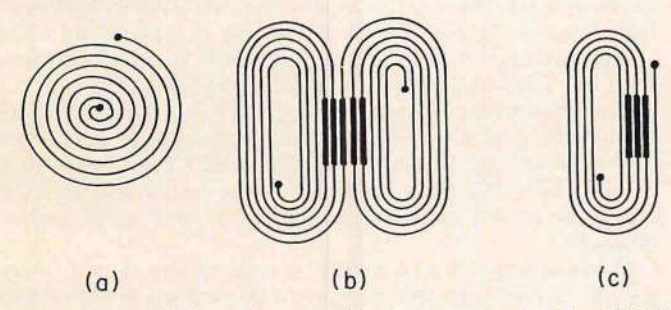


Figure 11—Efficient planar coils that can be used for EMAT construction: (a) spiral coil, (b) double-elongated spiral coil, and (c) single-elongated spiral coil. Frequently, all but the darkened central area of (b) or (c) is shielded or masked as shown in Fig. 12 so that an approximately linearly polarized current distribution can be induced in a metal surface.

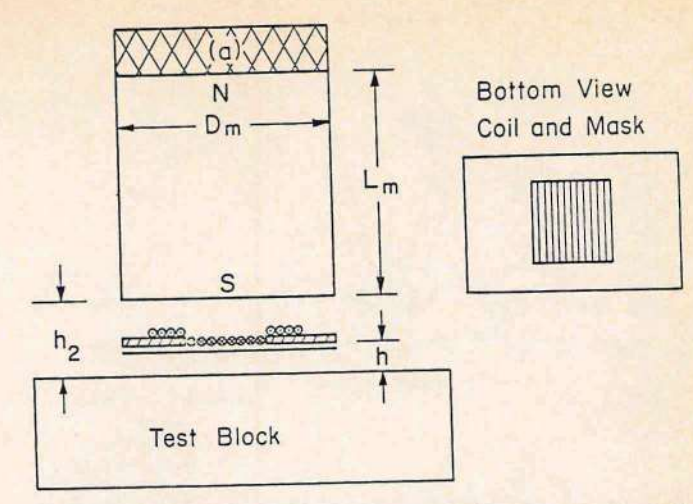


Figure 12—Pictoral representation of the construction of a linearly polarized shear wave permanent magnet EMAT.

TABLE 1ª

Metal	ρ _M (gm/cm³)	ρ μΩ-cm	v _s (trans) (cm/s)	V _s (long) (cm/s)	λ _s (trans) at 1 MHz (mm)	β	β (10 MHz)
6061 Al Alloy	2.7	4.5	3.0×10 ⁵	6.4×10 ⁵	3.0	0.083	0.25
Brass	8.6	7.0	2.1	4.7	2.1	0.25	0.80
Copper (Cu)	8.9	1.7	2.3	4.8	2.3	0.049	0.16
Nickel (Ni)	8.9	7.8	3.0	6.0	3.0	0.13	0.43
Iron (Fe)	7.8	10.0	3.2	6.0	3.2	0.15	0.49
Lead (Pb)	11.0	22.0	0.7	2.2	0.7	6.7	22.0
Steel	7.8	12.0	3.2	6.0	3.2	0.18	0.59
Tungster (W)	19.0	5.6	2.9	5.2	2.9	0.10	0.33

°Values for ρ_M , ρ , v_* (trans), and v_* (long) were obtained from either the Handbook of Chemistry and Physics, published by the Chemical Rubber Company, Edition 49, or the Handbook of Metals, published by the American Society of Metals, and are for polycrystalline materials near 20°C. λ_* (trans) is tabulated for transverse waves; λ_* (long) for longitudinal waves is about one half as large. The parameter $\beta = 4\pi^2 (\delta/\lambda_*)^2$; EMATs are only efficient as long as $\beta < 1$.

Permanent Magnet EMATs

By far the most compact bulk wave EMATs are constructed using rare-earth cobalt (RE-Co) permanent magnets (PMs) and coils, ¹⁸ such as shown in Fig. 11. The general construction of a PM EMAT is shown in Fig. 12, which also illustrates how a linearly polarized shear wave EMAT can be constructed. Typical values are Dm = Lm = 15 to 30 mm. When placed in a brass housing with a connector, these make a very rugged, compact ultrasonic transducer.

Reference to the curves in Figs. 13 and 14 show the importance of proper coil placement in making an efficient shear wave EMAT with a minimum in spurious longitudinal mode generation. Longitudinal wave PM EMATs have very low efficiency. As shown in Fig. 14, the radial component of the magnetic field (which is parallel to the surface) increases about linearly with radial distance. This component generates a longitudinal wave that one often wishes to minimize in a shear wave PM EMAT. Hence, the acceptable level of spurious mode generation determines the maximum coil size for any given magnet size.

Figure 13 shows that the normal component of the magnetic

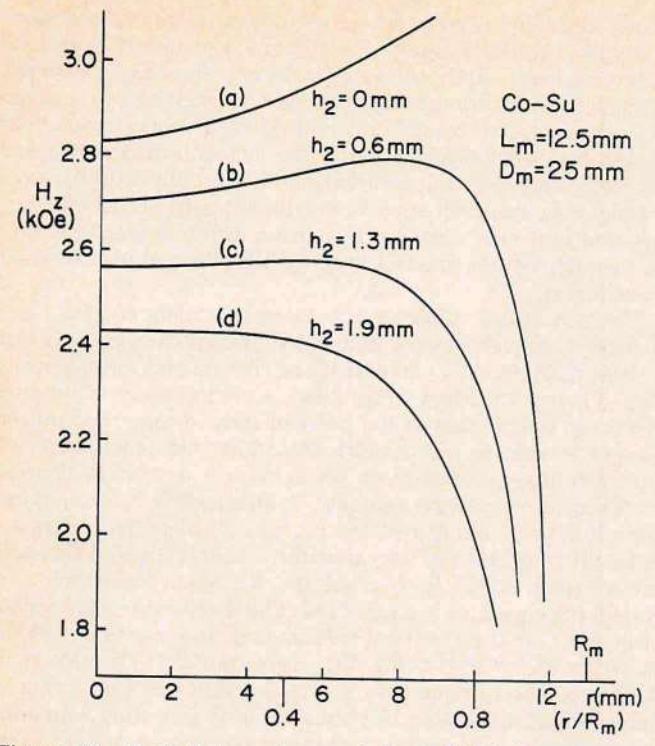


Figure 13—Radial dependence of the axial field component of a Co-Su permanent magnet.

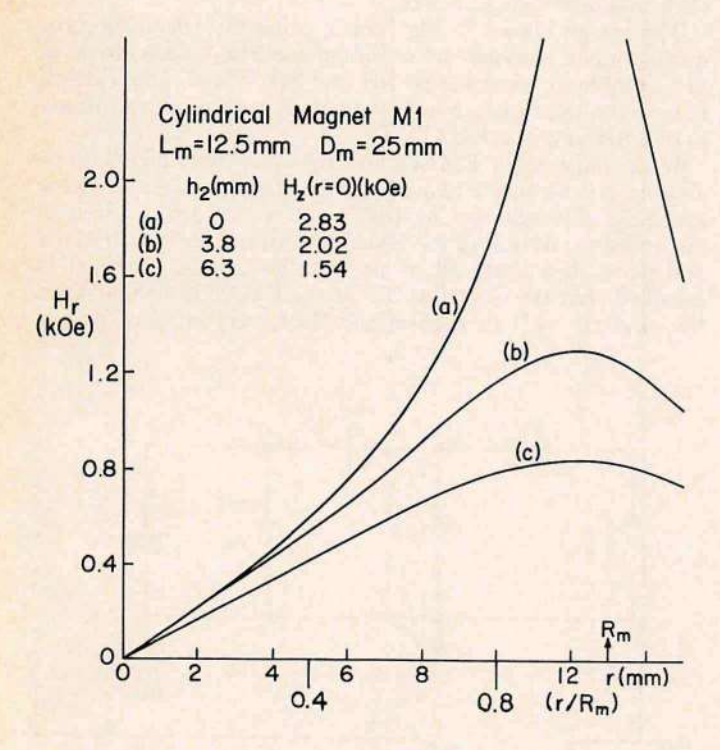


Figure 14—Radial dependence of the radial field component of a Co-Su permanent magnet.

field that generates a shear wave changes with both axial and radial distance. Therefore, a reasonably constant shear wave amplitude over the transducer active area again requires the coil size to be restricted. In order for the majority of the eddy currents to be generated in the metal under study, it is necessary to have the coil much closer to the test block surface than it is to the conducting magnet material. In fact, it is often desirable to place a conducting sheet on the pole nearest the coil so that eddy currents do not generate elastic waves by magnetostriction in RE-Co material. Normally, in a bulk wave

device, one places the coil one or two millimeters from the magnet pole face so that the EMAT will work well for lift-off distances of up to 0.3 mm.

Electromagnet EMATs

Although permanent magnets are compact, they are limited in both temperature and magnetic field. Temperature limitations will be discussed later. When working into a magnetic open circuit condition (infinite reluctance) such as shown in Fig. 12, all RE-Co PMs will yield surface magnetic fields less than 4.5 kilogauss^a (kG), and 3.5 kG is a more readily achievable value. When placed in a low reluctance magnetic circuit (the magnetic path closed with soft iron except for a small air gap), the gap field can reach at most the internal magnetic induction that is less than 10 kG. Fields obtainable with a 2 mm air gap are more generally limited to around 7 kG.

In some applications, the field obtainable using PMs may not be adequate. Another important consideration for ferromagnetic metals is getting the magnetic field normal to the surface, when one desires shear wave generation. Field lines are bent as they enter a ferromagnetic material with the change in angle depending upon the magnetic permeability. Large normal magnetic fields are usually advantageous when working with ferromagnetic metals because the permeability decreases with increasing field. One example of flux line bending upon entering a magnetic metal is shown in Fig. 15. In this example, an electromagnet of 15 000 ampere-turns produced a gap field of 10.6 kG for a gap of 5.0 mm. Beyond about one-half the pole radius, there is serious flux line bending leading to predominantly longitudinal wave generation via the Lorentz force mechanism and general elastic wave generation via magnetostriction.

Hence, even though electromagnets (EMs) can be large and cumbersome, there are many applications where one must consider their use. ^{17,19,20} It usually proves most convenient to package the coils for use with EMs in holders that are easily removed from the poles. These holders are often spring-loaded to facilitate good and reproducible coupling to the metal surface. For high-speed applications, it is important to have a very wear-resistant coil surface if the coil assembly rides in contact

^a1 gauss (G) · 0.0001=1 tesla (T). Thus, 4.5 kG · 0.1=0.45 T.

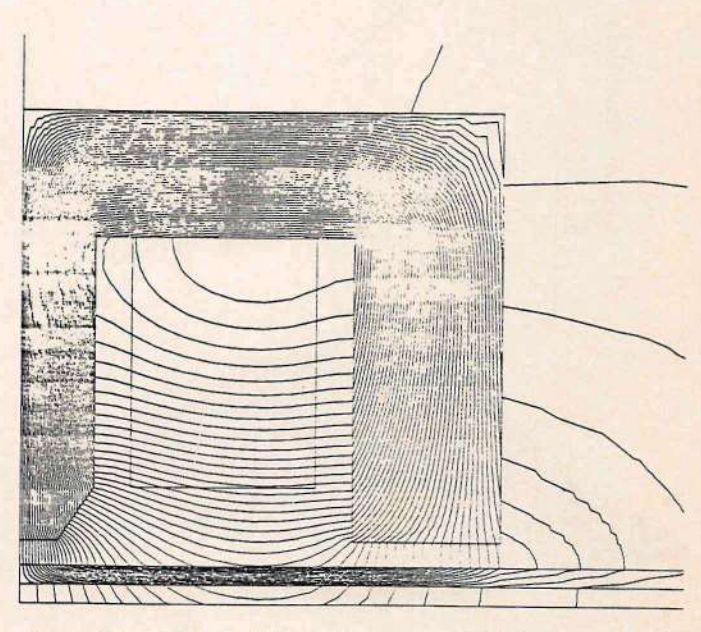


Figure 15—A plot of lines of constant field for a particular electromagnet design. Note how the field lines bend beneath each pole as they enter the magnetic base material.

with the metal surface. High-temperature applications will often require either cooling the pole caps or fabricating them from a high-temperature magnetic material.

Lift-off Effects and Mode Patterns

Figure 16a shows the measured lift-off dependence of the response of a 1.2 cm diameter spiral coil used with a 19 mm diameter RE-Co magnet. Most of the lift-off dependence is due to the decreasing eddy current intensity and not due to the bias field changes. This has the expected exponential behavior; the characteristic length is determined by the coil radius. Thus, lift-off effects can be minimized by using a coil of larger dimensions.

The amplitude distribution of induced current ²¹ for a lift-off equal to 0.2 of the radius of a spiral coil is shown in Fig. 16b. It is clear that the actual source size is a little larger than the coil radius.

DESIGN AND USE OF EMAT DRIVERS

To maximize the S/N for generation, both EMATs and piezoelectric transducers must be appropriately matched to ensure optimum utilization of the available driver output power. However, because piezoelectric transducers are generally much more efficient than EMATs and produce higher open-circuit voltages for a given surface displacement upon reception, the design of drivers for piezoelectric transducers has been generally determined by spectral considerations and the voltage-breakdown characteristics of semiconductor components used in capacitance-discharge circuits. The possibility of depoling a piezoelectric driver element must also be considered. As a consequence, resonant matching of piezoelectric transducers has not been widely used to maximize generation efficiencies in a narrow band of frequencies.

The electrical characteristics of most EMATs are signifi-

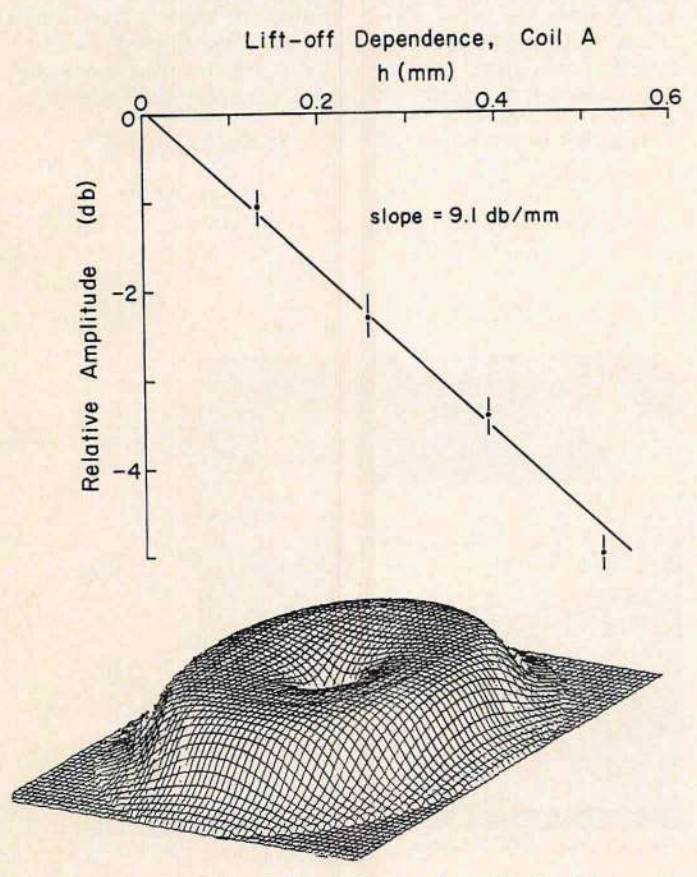


Figure 16—(a) Lift-off dependence of a spiral coil in a permanent magnet EMAT and (b) the current distribution induced by a spiral coil some distance above the surface.

cantly different from those of piezoelectric transducers normally used for NDE applications. EMATs generally behave as inductive loads, while the electrical input impedance of most piezoelectric transducers is dominated by the bulk capacitance of the piezoelectric crystal or ceramic drive element (reactances caused by mechanical motion of the elements themselves are generally only a small perturbation on the bulk capacitive reactance). As a consequence, to maximize transduction efficiencies and optimize temporal responses, different electrical circuit configurations must be used for EMATs and piezoelectric transducers.

The conceptual differences between electrical circuits used to drive most piezoelectric and EMAT transducer elements can be best illustrated by comparing the circuits and waveforms in Figs. 17 and 18. Figure 17a shows a rudimentary capacitive discharge circuit that is the basis of most commercial pulser designs for driving piezoelectric transducer elements. This circuit is composed of only six elements: (1) dc voltage source, V_c ; (2) current limiting resistor, R_c ; (3) ideal switch, S; (4) charging capacitor, C; (5) shunt resistor, RD; and (6) piezoelectric transducer, T. In operation, the capacitor C is first charged through the resistors Re and RD to a voltage, Ve. When the switch S is closed, the capacitor is discharged. The resultant voltage waveform, V(t), at the electrical terminals of the transducer, T, is shown in Fig. 20b. Initially, V(t) drops rapidly to a value that is approximately equal to -V_c. (In practice, this initial rate is determined by the nonideal behavior of S and other elements in the circuit.) Thereafter, V(t) increases monotonically to the ground potential as negative current flows through RD to balance the original charge Q = CVc that was on the capacitor. (It is assumed that R_c>>R_D.)

The circuit shown in Fig. 17a is primarily useful for producing only a unipolar drive voltage or current. This circuit is not suitable for multiperiod SH and ML EMAT applications but can be used quite successfully with bulk wave and single period SH and ML EMATs.

With multiperiod EMATs and in some other NDE applications, it is necessary to use gated bursts of rf current to drive an EMAT. For example, at least 4 cycles of rf are required to maximize the output of the EMAT shown in Fig. 2 when M=8 and when it is operated in an "end-fire" mode. (Here, it is assumed that the electrical "Q" of the EMAT is smaller than the acoustic "Q.") In such applications, very efficient pulsed

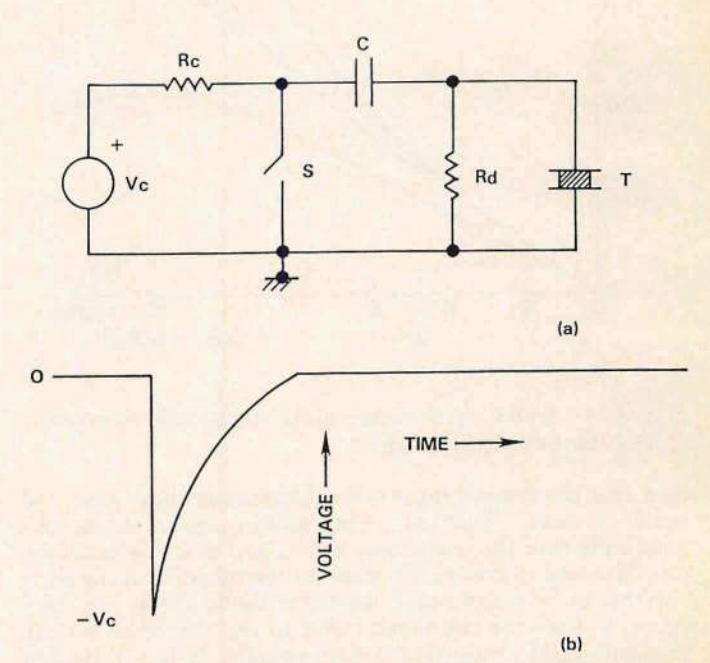


Figure 17—(a) Schematic for a circuit to excite a piezoelectric transducer T by the rapid discharge of capacitor C and (b) a typical waveform of the voltage across the transducer.

power amplifiers are needed. Fig. 18a shows an example of a highly functional circuit configuration that is inherently efficient and easily lends itself to tone-burst EMAT applications.

Technically, the circuit configuration shown in Fig. 18a is that of a complementary, voltage-switching Class-D power amplifier. This circuit also includes normal components that are needed for the practical implementation of EMATs. The components that are needed to ensure Class-D operation are the constant voltage sources \pm V_B, the two ideal switches S₁ and S₂, and the series tank circuit composed of the EMAT inductance and external capacitor, C₄. The waveforms associated with the operation of a rudimentary Class-D amplifier are shown in Fig. 21b.

The circuit shown in Fig. 18a operates as follows. The switches S₁ and S₂ are alternately closed and opened at a fundamental frequency, f₀. Ideally, each switch operates at a 50 percent duty cycle. As a result of this commutating action, a "square-wave" voltage waveform V(t), shown in Fig. 18b, appears at the output of the amplifier at "O." The series tank circuit mentioned above acts as a filter that presents the minimum impedance to the fundamental component of the applied voltage waveform. Ideally, the symmetry of the network in Fig. 18a ensures that the dc and even harmonic terms of the Fourier series associated with the driving voltage waveform are not present. The resultant current waveform I(t) is also shown in Fig. 18b. Note that I(t) is nearly sinusoidal and free of evenorder harmonic components.

This circuit configuration is highly efficient because little power is dissipated by the switches and a damping resistor is not used. The switches dissipate little power because they drop a very small voltage while passing the maximum current. When implemented with practical switching devices, the performance of the circuit is, of course, subject to the effects of saturation, parasitics, finite switching-times, and device breakdown considerations.

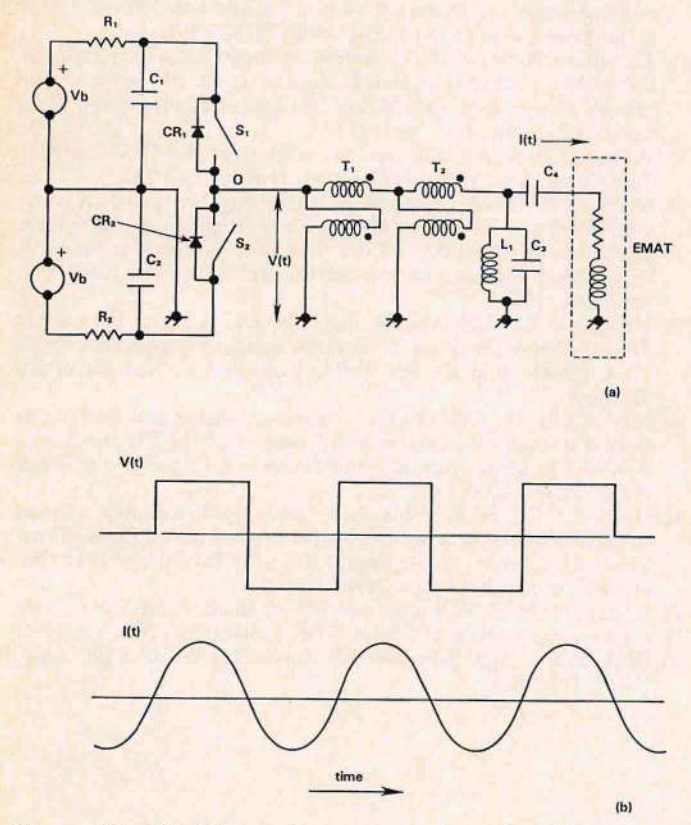


Figure 18—(a) Schematic representation of a Class-D amplifier that can be used for the tone-burst excitation of an EMAT plus some practical circuitry needed to match the EMAT to the amplifier and (b) typical amplifier output voltage and EMAT current waveforms.

Because of practical considerations associated with break-down characteristics of semiconductor switching elements and input impedance characteristics of typical EMATs, the circuit shown in Fig. 18a includes the following additionial components: current limiting resistors, R_1 and R_2 ; storage capacitors, C_1 and C_2 ; protection diodes, CR_1 and CR_2 ; impedance matching transformers, C_1 and C_2 ; and a parallel tank circuit consisting of C_1 and C_3 .

The role of the capacitor-resistor networks R_1 - C_1 and R_2 - C_2 is to provide sufficient energy for short rf bursts at the fundamental frequency, f_o . In the event of a short circuit, resistors R_1 and R_2 limit the output current. Diodes CR_1 and CR_2 provide a path for reverse currents when either S_1 or S_2 are in the off position. The two transformers reduce the input impedance of the EMAT (tuned to frequency f_o by C_4) to better match the low impedance levels of the Class-D output stage while the tank circuit (L_1 - C_3) provides a bypass to ground for higher-than-fundamental harmonies.

Figure 19 shows a circuit diagram of a practical though not state-of-the-art Class D amplifier designed to operate in the 300 to 600 kHz frequency range. This amplifier is capable of producing peak outputs in the range of 1500 watts (W) when used in conjunction with an SH wave EMAT such as is shown in Fig. 4 and having four periods. Both transformers T, and T2 are wound using eight turns of a small diameter, flexible coaxial cable on 9.3 mm outside diameter "Q-1" type ferrite cores. The amplifier shown in Fig. 19 consumes approximately 6 W average power when operated at a 0.4 percent duty cycle. As expected, the current waveform at f_o = 450 kHz is sinusoidal; the peak-to-peak current is 80 amperes (A). However, the voltage waveform is not square. This is caused by the finite switching time of the high-power bipolar transistors used to implement the switches S1 and S2. At 250 kHz, the output voltage waveform becomes square. The amplifier in Fig. 19 was implemented using high-power, bipolar switching transistors because metal-oxide semiconductor field-effect transducer (MOSFET) devices with comparable breakdown characteristics were not available when this circuit was initially designed. The new power MOSFET technology has been used to implement switches S1 and S2 with successful operation up to 5 MHz. Below 2 MHz, peak power output up to at least 10 kW can be realized.

It is also possible to use high-power pulsed oscillators or gated amplifiers as EMAT drivers, but ringing of tuned output stages can place severe restrictions on the recovery time that can be realized by the EMAT system.

RECEIVERS FOR USE WITH EMATS

Noise figure and overload recovery time are the main considerations for EMAT receiver/preamplifiers. When used in the single transducer, pulse-echo mode, the preamplifier must be able to withstand the full driver voltage connected to the EMAT and then to recover rapidly so that flaw reflections or backsurface signals can be measured. The input protection circuit shown in Fig. 20 is normally adequate to allow an amplifier to

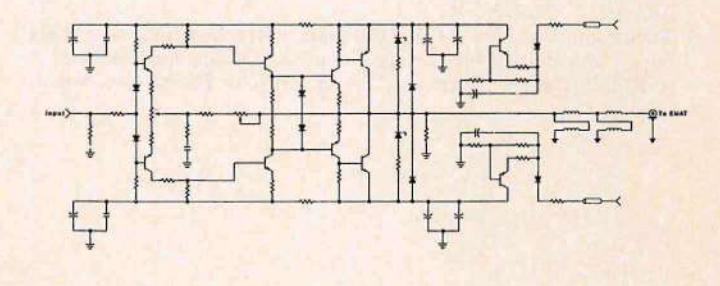


Figure 19—Schematic of a bipolar transistor EMAT power amplifier.

EMAT POWER AMPLIFIER

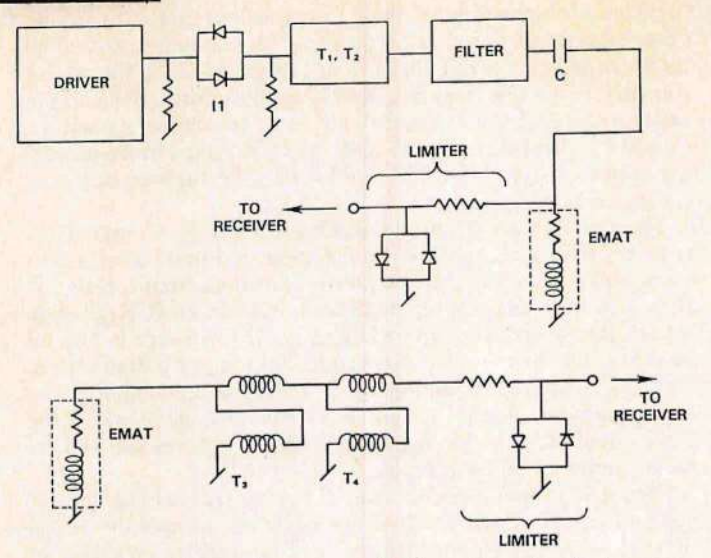


Figure 20-Schematic representation of methods for connecting an EMAT to a receiver/preamplifier.

tolerate up to 1 kV applied across the EMAT and yet recover within 3 microseconds (µs) after the drive current is removed. When tuned output drivers are used, a series diode isolator, shown as I1 in Fig. 20a, must be used to obtain both voltage and capacitive isolation between the driver and receiver.

When used only as a receiver, the receiver input circuitry need not withstand the drive voltage. Under these circumstances, it is easy to use matching transformers T3 and T4 to obtain a better noise figure. It is also possible to use similar transformers in a pulse-echo setup, but care must now be taken in choosing the absolute impedance levels of the EMAT, T3 and T4; otherwise, much valuable drive current will be shunted past the EMAT.

CONCLUSION

The design and construction of SH wave and bulk shear and longitudinal wave EMATs has been described. EMATs will always be less efficient than some of the other means of generating elastic waves. EMATs can now be used with properly designed instrumentation for thickness gaging and defect detection. Consequently, their use should be considered whenever it is apparent that features such as the absence of fluid couplants, high-temperature operation, normal shear wave generation, control of shear wave polarization control, high-speed scanning, and electronically steerable bulk waves are desired.

References

- 1. Maxfield, B. W., and J. K. Hulbert, "Electromagnetic Acoustic Wave Transducers (EMATs): Their Operation and Mode Patterns," published in the Proceedings of the 10th Symposium on NDE, San
- Antonio, TX, 1975, p 44. 2. Thompson, R. Bruce, "The Relationship Between Radiating Body Forces and Equivalent Surface Stresses: Analysis and Application to EMAT Design," Journal of Nondestructive Evaluation, Vol. 1, 1980, p 79.

- 3. Pardee, William J., and R. B. Thompson, "Half-Space Radiation by EMATs," Journal of Nondestructive Evaluation, Vol. 1, 1980, p 157.
- 4. Thompson, R. Bruce, "A Model for the Electromagnetic Generation and Detection of Rayleigh and Lamb Waves," IEEE Transactions on Sonics and Ultrasonics, Vol. SU-20, 1973, p 340.
- 5. Gaerttner, M. R., W. D. Wallace, and B. W. Maxfield, "Experiments Relating to the Theory of Magnetic Direct Generation of Ultrasound in Metals," Physics Review, Vol. 184, 1969, p 702.
- 6. Vasile, C. F., and R. B. Thompson, "Evaluation of Electromagnetic-Acoustic Concepts of Inspection of Steam Generator Tubing," EPRI Report No. NP-519. Electric Power Research Institute, Palo Alto, CA.
- 7. Fortunko, C. M., and R. E. Schramm, "Ultrasonic Nondestructive Evaluations of Butt Welds Using Electromagnetic-Acoustic Trans-
- ducers," Welding Journal, Feb. 1982, p 39. 8. Martin, J. F., and R. B. Thompson, "The Twin-Magnet EMAT Configuration for Exciting Horizontally Polarized Shear Waves," IEEE Ultrasonics Symposium Proceedings, 1981, p 388. Institute of Electrical and Electronics Engineers, New York, NY.
- 9. Szabo, Thomas L., "Advanced SAW Electromagnetic Transducer Design," IEEE Ultrasonics Symposium Proceedings, 1976, p 29. Institute of Electrical and Electronics Engineers, New York, NY.
- 10. Frost, H. M., T. L. Szabo, and J. C. Sethares, "The Flat Conductor Electromagnetic SAW Transducer: Theory and Experiment," IEEE Ultrasonics Symposium Proceedings, 1975, p 601. Institute of Electrical and Electronics Engineers, New York, NY.
- 11. Fortunko, C. M., "Ultrasonic Inspection of Weldments with Frequency Scanned SH Waves," IEEE Ultrasonics Symposium Proceedings, 1979, p 253. Institute of Electrical and Electronics Engineers, New York, NY.
- 12. Fortunko, C. M., and J. C. Moulder, "Ultrasonic Inspection of Stainless Steel Butt Welds Using Horizontally Polarized Shear Waves, Ultrasonics, May 1982, p 113.
- Vasile, C. F., and R. B. Thompson, "Excitation of Horizontally Polarized Elastic Waves by Electromagnetic Transducers with Periodic Magnets," Journal of Applied Physics, Vol. 50, 1979, p 2583.
- 14. Fortunko, C. M., "Ultrasonic Detection and Sizing of Two-Dimensional Defects at Long Wavelengths," Applied Physics Letters, Vol. 38, 1981, p 980.
- 15. Salzburger, H. J., "Defect Characterization by Multimode Testing of Steel Strips and Plates with e.m.a. Excited Lamb Waves," Proceedings of Ultrasonics International, 1979, p 404.
- 16. Thompson, R. Bruce, "Electromagnetic Generation of Rayleigh and Lamb-Waves in Ferromagnetic Materials," IEEE Ultrasonics Symposium Proceedings, 1975, p 633. Institute of Electrical and Electronics Engineers, New York, NY.
- 17. Whittington, K. R., "Ultrasonic Inspection of Hot Steel," British Journal of Non-Destructive Testing, Sept. 1978, p 242.
- 18. Maxfield, B. W., M. Linzer, W. B. McConnaughey, and J. K. Hulbert, "Design of Permanent Magnet Electromagnetic Acoustic-Wave Transducers (EMATs)," IEEE Ultrasonics Symposium Proceedings, 1976, p 22. Institute of Electrical and Electronics Engineers, New York, NY.
- 19. Miyagawa, K., Y. Sasaki, N. Matsuda, and S. Sato, "Ultrasonic Testing of Steel Products by Electromagnetic Transducers," Paper 4H-4, presented at the 9th World Conference on Nondestructive Testing
- 20. Maxfield, B. W., "EMATs for Thickness Gauging and Defect Detection in Boiler Tubing," paper presented at the Electric Power Research Institute Workshop on Failures and Inspections of Fossil Boiler Tubes, April 1983.
- 21. Hulbert, J. K., and B. W. Maxfield, "Intensity Distribution of Shear Acoustic Waves Scattered by a Flat-Bottomed Hole," IEEE Ultrasonics Symposium Proceedings, 1976, p 70. Institute of Electrical and Electronics Engineers, New York, NY.
- Krauss, H. L., C. W. Bortian, and F. H. Raab, Solid-State Radio
- Engineering, 1980, p 432. John Wiley & Sons, Inc., New York, NY. 23. Raab, F. H., "High Efficiency RF Power Amplifiers," Ham Radio, Vol. 7, 1974, p 8.